Dalton Transactions

COMMUNICATION

View Article Online
View Journal | View Issue

Cite this: *Dalton Trans.*, 2016, **45**, 474

Received 21st October 2015,
Accepted 18th November 2015

DOI: 10.1039/c5dt04138d

www.rsc.org/dalton

Nickel(II) complexes of *N*-CH_2CF_3 cyclam derivatives as contrast agents for ^{19}F magnetic resonance imaging†

Jan Blahut,[a] Petr Hermann,[a] Andrea Gálisová,[b] Vít Herynek,[b] Ivana Císařová,[a] Zdeněk Tošner[c] and Jan Kotek*[a]

Kinetically inert Ni(II) complexes of N^1,N^8-bis(2,2,2-trifluoroethyl) cyclams with hydrogen atoms or phosphonic acid groups in the N^4,N^{11}-positions show significant ^{19}F NMR relaxation rate enhancement useful for 19-fluorine MRI imaging.

Magnetic resonance imaging (MRI) is one of the most common techniques in molecular imaging. It is based on the detection of the NMR signal originating from water protons in a tissue. To increase its sensitivity, paramagnetic contrast agents (CAs) are often applied.[1,2] They affect mainly the longitudinal (T_1) relaxation time of the ^1H signal, which leads to an increase in the intensity of the water proton MRI signal. However, essentially all tissues contain water and, thus, the background signal compromises the detection accuracy. This problem can be solved by using non-proton MRI and the ^{19}F nucleus seems to be the most promising candidate.[3–6] Natural monoisotopic ^{19}F has an NMR resonance frequency close to that of ^1H (40.08 MHz T^{-1} for ^{19}F compared to 42.58 MHz T^{-1} for ^1H) and exhibits sensitivity comparable to ^1H (83%). Fluorine concentration in organisms is virtually zero and, therefore, the lack of background in fluorine-based images enables "hot-spot" imaging. The wider spectral range of the ^{19}F nucleus (~350 ppm) compared to ^1H (~10 ppm) is also beneficial for some applications. Moreover, only small hardware and software adjustments of standard ^1H scanners are needed for ^{19}F detection.[6] This makes the nucleus very potent for *e.g.* cellular tracking of labelled cell cultures.[7–11]

However, the ^{19}F nucleus present in organic molecules has usually a very long T_1 relaxation time requiring a long delay between excitation pulses; this prolongs the total duration of imaging experiments to unrealistic lengths. Shortening of the T_1 relaxation time can result in significant shortening of the experimental time. However, it is necessary to take into account the concomitant shortening of the transversal (T_2 or T_2^*) relaxation time, which leads to signal broadening and can result in very fast loss of signal intensity. It has been shown that the introduction of highly paramagnetic lanthanide(III) ions to the close vicinity of the fluorine atom(s) leads to significant shortening of the relaxation times,[12] and the T_2^*/T_1 ratio is in the range of 0.3–0.9, which is suitable for MRI measurements.[12c,13]

It is known that, despite the low overall electronic spin (S = 1) and magnetic momentum (μ_{eff} ~ 3 B.M.) of Ni(II), this ion can induce a large paramagnetic chemical shift and relaxation enhancement comparable to that of lanthanide(III) ions with higher S and μ.[14] Therefore, some Ni(II) complexes have been studied as MRI agents employable in the Chemical Exchange Saturation Transfer method.[15] Here, we decided to study the ^{19}F NMR relaxation properties of Ni(II) complexes. The Ni(II) ion fits perfectly in the cavity of 1,4,8,11-tetraazacyclotetradecane (cyclam) and cyclam derivatives are well-known to form Ni(II) complexes with high thermodynamic stability, especially with ligands having coordinating pendant arms enabling octahedral binding to the metal. The 2,2,2-trifluoroethyl side arm was chosen as a group containing a high number of equivalent fluorine atoms. Therefore, ligands **1** and H_4te2p-tfe$_2$ (Fig. 1)

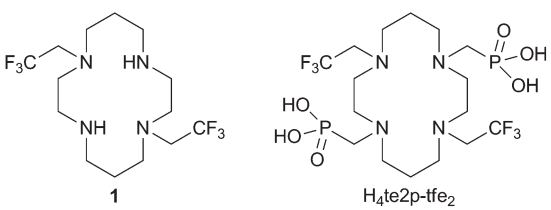

Fig. 1 Ligands studied in this work.

[a]*Department of Inorganic Chemistry, Faculty of Science, Charles University (Univerzita Karlova), Hlavova 2030, 128 43 Prague 2, Czech Republic. E-mail: modrej@natur.cuni.cz; Fax: +420-221951253; Tel: +420-221951261*
[b]*Department of Radiodiagnostic and Interventional Radiology, Magnetic Resonance Unit, Institute for Clinical and Experimental Medicine, Vídeňská 1958/9, Prague 4, 140 21 Czech Republic*
[c]*NMR Laboratory, Faculty of Science, Charles University (Univerzita Karlova), Hlavova 2030, 128 43 Prague 2, Czech Republic*

†Electronic supplementary information (ESI) available: Synthesis of studied compounds, single-crystal RTG diffraction data, details on potentiometric study, study of acid-assisted dissociation of prepared complexes, relaxation study, $^1H/^{19}F$ MRI visualization. CCDC 1430237–1430242. For ESI and crystallographic data in CIF or other electronic format see DOI: 10.1039/c5dt04138d

were suggested for testing the ^{19}F NMR parameters of their complexes.

Acylation of 1,8-dibenzylcyclam with ethyl trifluoroacetate or trifluoroacetic anhydride yielded the corresponding bis(amide). It was followed by BH_3 reduction[16] in diglyme at elevated temperature and the benzyl protecting groups were removed by Pd/C hydrogenolysis to obtain ligand **1**. The reaction[17] of amine **1** in neat $P(OEt)_3$ with CH_2O led to the tetraethyl bis(methylenephosphonate) cyclam derivative. The ethylester groups were removed by transesterification with trimethylsilylbromide[18] followed by the silylester hydrolysis to yield H_4te2p-tfe$_2$, which was isolated in a zwitterionic form after ion exchange chromatography. Synthetic details and results of a single-crystal X-ray diffraction study of **1**·2HCl·2H_2O and H_4te2p-tfe$_2$·4HBr·0.5H_2O are given in the ESI (Fig. S5 and S6†).

Ligand **1** (in the form of a hydrochloride) reacts with Ni(II) salts in aqueous solutions to give a light greenish-blue precipitate. The structure of this compound was determined by a single-crystal X-ray study as *cis*-[Ni(**1**)$(Cl)_2$] (see ESI Fig. S7†); the central ion is surrounded by four cyclam nitrogen atoms in the *cis*-V configuration[19] with two-fold symmetry (d_{Ni-N} = 2.10 and 2.26 Å for secondary and tertiary amines, respectively) and *cis*-chloride anions coordinated with d_{Ni-Cl} = 2.42 Å.

However, the *cis*-[Ni(**1**)$(Cl)_2$] complex shows extremely low solubility in all solvents. Thus, the presence of chloride ions had to be avoided during the preparation of a water-soluble complex. Therefore, ligand **1** in the form of a free base and $Ni(ClO_4)_2$ was used for further complex preparation. The course of the reaction in the H_2O : DMSO 1 : 6.5 mixture at 50 °C was followed by ^{19}F NMR spectroscopy (Fig. S2†). Such a solvent mixture was used to keep the reaction mixture fully homogeneous right from the beginning as compound **1** is poorly soluble in water. The reaction proceeds (at 50 °C) through an intermediate (δ_F = −22.9 ppm) and is completed during 90 min to give the final complex with δ_F = −29.3 ppm (at 50 °C). On cooling to 25 °C, the signal shifts to −26.5 ppm. No further ^{19}F NMR spectral changes were observed upon heating the solution at 100 °C for several days.

To obtain an aqueous stock solution, prolonged heating (80 °C) of the suspension of ligand **1** with $Ni(ClO_4)_2$ in H_2O : MeOH 1 : 1 (with subsequent evaporation of MeOH) was used. It led to the formation of a light blue aqueous solution of a single product with δ_F = −26.2 ppm. When the aqueous solution of the complex prepared in H_2O : MeOH was mixed with the sample prepared in H_2O : DMSO, only one symmetric signal in ^{19}F NMR was observed revealing that the species formed in both experiments are identical complexes.

Despite a number of attempts, we were not able to crystallize this light blue product. However, red single-crystals of *trans*-[Ni(**1**)]$(ClO_4)_2$ (Fig. 2) were obtained when the blue aqueous solution of the complex was saturated with $NaClO_4$ and was left standing for a few weeks. In this complex, the cyclam ring is coordinated in the centrosymmetric *trans*-III configuration[19] (d_{Ni-N} = 1.95 and 1.99 Å for secondary and tertiary amino groups, respectively). Consistent with the red colour, only very weak axial interaction with perchlorate anions located in distant positions (d_{Ni-O} = 2.83 Å) was observed.

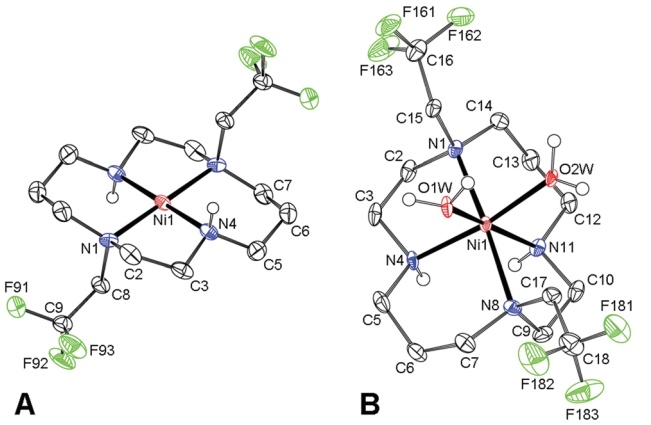

Fig. 2 Structures of (A): *trans*-[Ni(**1**)]$^{2+}$ and (B): *cis*-[Ni(**1**)$(H_2O)_2$]$^{2+}$ complex cations found in the solid state structures of *trans*-[Ni(**1**)]$(ClO_4)_2$ and *cis*-[Ni(**1**)$(H_2O)_2$](TsO)$_2$, respectively. Carbon-bound hydrogen atoms are omitted for clarity. Thermal ellipsoids are shown at the 60% probability level.

Dissolution of the red *trans*-[Ni(**1**)]$(ClO_4)_2$ complex in water produced a light blue solution with δ_F = −19.3 ppm and the species slowly isomerizes with first-order kinetics ($\tau_{1/2}$ ~3.5 h, 25 °C) to a species with δ_F −26.3 ppm (Fig. S3†). The final species is identical to the original Ni(II)–**1** complex, as it was confirmed by ^{19}F NMR after the addition of a standard. Taking into account the isomerism of metal ion–cyclam complexes,[19] red *trans*-[Ni(**1**)]$(ClO_4)_2$ with the *trans*-III configuration probably forms a blue hexacoordinated *trans*-[Ni(**1**)$(H_2O)_2$]$^{2+}$ species upon dissolution, and this complex is rearranged in solution to the *cis*-[Ni(**1**)$(H_2O)_2$]$^{2+}$ species with the *cis*-V cyclam conformation.

Typically, the *trans*-III isomer of cyclam complexes is considered to be the thermodynamically most stable one,[20] and the preference of the *cis*-V cyclam conformation for the Ni(II)–**1** complex is rather surprising. However, the higher stability of the *cis*-V isomer over the *trans*-III one was supported also by the isolation of *cis*-[Ni(**1**)$(H_2O)_2$](TsO)$_2$ (Fig. 2). The structure shows Ni–N distances of 2.07 and 2.09 Å for secondary amino groups, and 2.22 and 2.25 Å for tertiary ones, respectively, with two water molecules coordinated with d_{Ni-O} = 2.07 and 2.10 Å.

Based on the data presented above, one can conclude that the reaction of ligand **1** with $Ni(ClO_4)_2$ leads to the formation of the *cis*-[Ni(**1**)$(H_2O)_2$]$(ClO_4)_2$ complex. The geometries of Ni(II) coordination polyhedra found in the solid state structures are compiled in Table S2† and are comparable to other [Ni(L)$(H_2O)_2$] complexes of cyclam derivatives.[21,22] The Ni–F distances found in all solid-state structures were in the range of 4.8–5.4 Å (Table S3†).

The complex of the second studied ligand, H_4te2p-tfe$_2$, was prepared by heating the ligand together with a slight excess of

$NiCl_2$ in aq. ammonia (pH 10) at 75 °C for 24 h; the excess of Ni(II) ions was removed by column chromatography. As mentioned above, the course of the reaction was followed by ^{19}F NMR (Fig. S4†), which showed a fast drop in the concentration of the free ligand (δ_F = −68.3 ppm), and the formation of an intermediate (δ_F = −41.1 ppm) and its slower rearrangement to the final product (δ_F = −26.4 ppm). The time-dependence of intensities of all three signals could be satisfactorily fitted using a monoexponential function (Fig. S4†) and showed comparable rate constants for all three processes (see the ESI†). Such behaviour points to the presence of an equilibrium between the free ligand and the intermediate with an irreversible (rate-determining) reaction step leading to the formation of the final complex.

The final product was isolated in the form of light blue crystals, which were identified as $(NH_4)\{trans$-[Ni(Hte2p-tfe$_2$)]$\}\cdot 3.25H_2O$ by single-crystal X-ray diffraction. Therefore, the complex species present in solution are expected to be *trans*-$[Ni(H_nte2p\text{-}tfe_2)]^{n-2}$ (n = 0, 1) depending on pH. The molecular structure of the complex anion is shown in Fig. 3, and geometric parameters of the coordination sphere of Ni(II) and Ni–F distances are listed in Tables S2 and S3.† The cyclam ring exhibits the *trans*-III configuration[19] (d_{Ni-N} are ~2.10 and 2.11 Å for amino groups bearing the methylenephosphonate pendant arms, and 2.22 and 2.23 Å for those substituted by trifluoroethyl groups) with the oxygen atoms of phosphonate groups occupying apical positions (Ni–O distances are 2.06 and 2.10 Å, respectively). The molecules of the complex are connected *via* short hydrogen bonds between the oxygen atoms of protonated and unprotonated phosphonate pendants ($d_{O\cdots O}$ = 2.47 Å), forming infinite chains, similar to what was found for analogous complexes of cyclam-methylenephosphonate derivatives.[23,24] Bonding distances and the overall molecular structure are very similar to those of Ni(II) complexes of analogous derivatives.[22,24]

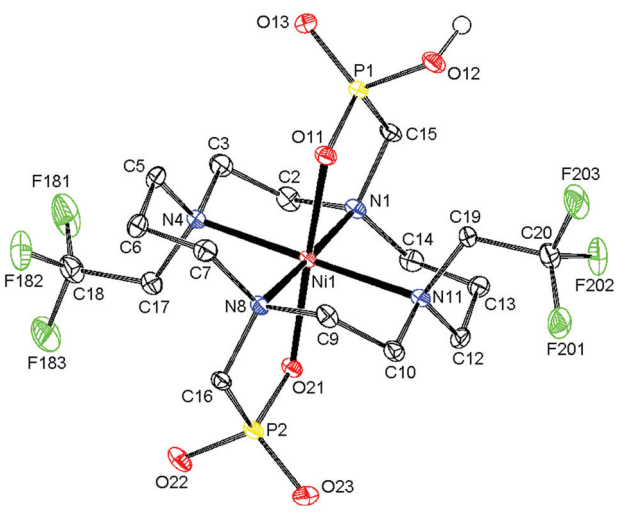

Fig. 3 Molecular structure of the *trans*-$[Ni(Hte2p\text{-}tfe_2)]^-$ anion found in the crystal structure of *trans*-$(NH_4)[Ni(Hte2p\text{-}tfe_2)]\cdot 3.25H_2O$. Carbon-bound hydrogen atoms are omitted for clarity. Thermal ellipsoids are shown at the 60% probability level.

The thermodynamics of complexing properties of the phosphonate H_4te2p-tfe$_2$ ligand was studied by potentiometry (see the ESI and Table S4†). The comparison of ligand stepwise protonation constants ($\log K_{1-4}$ 10.86, 10.09, 5.60 and 4.73) with those of the N^1,N^8-dimethyl-N^4,N^{11}-bis(methylenephosphonate) analogue[25] ($\log K_{1-4}$ 11.47, 12.17, 7.20 and 6.33, Table S5†) points to significantly decreased ligand basicity caused by the presence of electron-withdrawing $-CH_2CF_3$ groups. Surprisingly, it affects not only the first two protonation constants corresponding to the ring amino groups but also those of the phosphonate moieties, probably as a result of a strong electron-withdrawing effect transferred through intramolecular hydrogen bonds, which are expected to have a geometry analogous to that found for related cyclam derivatives.[25] Equilibration of the Ni(II)–H_4te2p-tfe$_2$ system is relatively slow and, therefore, the out-of-cell titration method had to be used. As the complexation mechanism is not fully straightforward (see above), the samples used for the out-of-cell titration were heated at 50 °C for 2 weeks to ensure quantitative rearrangement of the intermediate to the final *trans* isomer. The time required for equilibration was checked by ^{19}F NMR of separate samples. The stability constant, $\log K_{NiL}$ = 13.28, is about 2–7 orders of magnitude lower than the constants of complexes with related ligands (Table S5†),[26,27] mainly as a consequence of the lower ligand basicity. The distribution diagram of the system (Fig. S8†) shows that full Ni(II) complexation by H_4te2p-tfe$_2$ is completed at pH 7 and the complex is present at this pH almost entirely in a fully deprotonated form.

For possible *in vitro*/*in vivo* utilization, kinetic inertness is a more important parameter than thermodynamic stability. Kinetic inertness is often tested in acidic solutions as acid-assisted complex dissociation. Thus, the decomposition of both studied complexes was examined in 1 M aq. HCl at 37 and 80 °C. Both complexes are decomposed relatively slowly by HCl at 37 °C ($\tau_{1/2}$ ~8 and ~10 h for *cis*-$[Ni(\mathbf{1})(H_2O)_2]^{2+}$ and *trans*-$[Ni(H_nte2p\text{-}tfe_2)]^{n-2}$, respectively) but the decomplexation of the *cis*-$[Ni(\mathbf{1})(H_2O)_2]^{2+}$ complex is substantially accelerated at the higher temperature (80 °C, $\tau_{1/2}$ ~ 3 min compared to ~5 h for *trans*-$[Ni(H_nte2p\text{-}tfe_2)]^{n-2}$, Table S6†), as the presence of apically coordinated pendant arms in the H_4te2p-tfe$_2$ complex enhances kinetic inertness. High inertness has been observed for several Cu(II) complexes with analogous cyclam-based ligands,[28] and highly protonated species of several Ni(II)[22,24] complexes of phosphonated cyclam derivatives have been isolated even in the solid state. These results suggest sufficient complex stability under physiological conditions and warrant the possible use of the Ni(II)–H_4te2p-tfe$_2$ complex in *in vitro*/*in vivo* applications.

As the *trans*-$[Ni(te2p\text{-}tfe_2)]^{2-}$ complex is kinetically inert and promises reasonable stability *in vivo*, its ^{19}F MRI-related parameters were investigated. Although the *cis*-$[Ni(\mathbf{1})(H_2O)_2]^{2+}$ complex is not suitable for any *in vivo* application due to its low solubility in chloride-containing media, it was studied as well for comparative purposes as there are no related data

reported in the literature at all. The ^{19}F NMR relaxation measurement of both Ni(II) complexes at B_0 = 7.05 T showed extreme shortening of ^{19}F NMR T_1 relaxation times by 2–3 orders of magnitude compared with the values observed for the free ligands, **1** and H_4te2p-tfe$_2$ (Table 1).

The suitability of the *trans*-[Ni(te2p-tfe$_2$)]$^{2-}$complex for ^{19}F MRI was tested by phantom visualization at B = 4.7 T. At this magnetic field, the T_1 of the complex is very short in the millisecond range with a still convenient T_2^*/T_1 relaxation times ratio (Table 1). The observed relaxation times are even slightly shorter than those reported for studied Ln(III) complexes – in the cases of highly paramagnetic Tb(III), Dy(III) and Ho(III) complexes with the estimated Ln(III)–F distance lying in the range of 5–7 Å, the reported T_1 is typically in the range of 7–11 ms at 4.7 T and room temperature.[12c,13] The very short relaxation time of the Ni(II) complex required optimization of the fast pulse sequence – for the visualization of the complex, a fast gradient echo sequence with TE = 1.3 ms and TR = 3 ms was used. The slowly relaxing samples (containing the free ligand and trifluoroethanol used as a standard) were best measured using a long turbospin echo sequence employing TE = 40 ms and TR = 2000 ms. For localization of the samples, the ^{1}H MRI scan (Fig. 4A) was also acquired. Fig. 4 shows the results of the MRI visualization. The brightness of aq. solution of the Ni(II) complex compared to aq. solutions of the free ligand and trifluoroethanol is caused by its paramagnetism, which shortens the T_1 relaxation time of water protons (r_1(complex) = 0.12 mm^{-1} s^{-1}, 4.7 T, 25 °C). As each sample has a different ^{19}F NMR chemical shift (δ_F −26 ppm, −68 ppm and −77 ppm for the complex, free ligand and trifluoroethanol, respectively), each signal can be excited separately. In the case of the fast sequence, only a negligible signal of the free ligand was detected, as virtually no diamagnetic sample relaxation occurs during the sequence time-scale. On the contrary, in the experiment employing the long sequence, no signal of the paramagnetic sample was found as its magnetization relaxes before the start of acquisition.

The samples of free ligand **1** and *cis*-[Ni(**1**)(H$_2$O)$_2$](ClO$_4$)$_2$ show fully concordant behaviour (Fig. S9†).

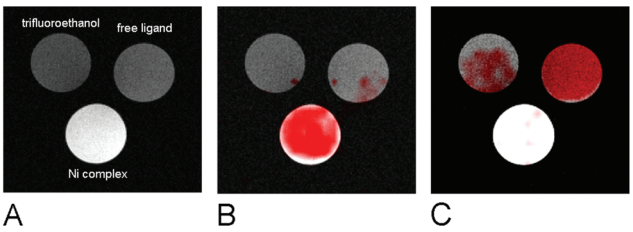

Fig. 4 MRI study of phantoms containing trifluoroethanol, free H_4te2p-tfe$_2$ and the *trans*-[Ni(te2p-tfe$_2$)]$^{2-}$ complex (c_F = 0.004 M in all samples), B = 4.7 T, 25 °C, home-made ^{1}H/^{19}F surface single loop coil. (A) ^{1}H MRI scan, gradient echo sequence, flip angle 30°, TE = 3.7 ms, TR = 100 ms, matrix 256 × 256. (B) Overlay of ^{1}H MRI with ^{19}F MRI; ^{19}F MRI was optimized for the complex; acquired at δ = −26 ppm, gradient echo sequence, TE = 1.3 ms, TR = 3 ms, matrix 32 × 32 interpolated to 256 × 256. (C) Overlay of ^{1}H MRI with ^{19}F MRI; ^{19}F MRI was optimized for the ligand; acquired at δ = −77 ppm, turbospin echo sequence, TE = 40 ms, TR = 2000 ms, matrix 32 × 32 interpolated to 256 × 256.

In conclusion, transition metal ion complexes of fluorine-containing ligands can be considered a new class of ^{19}F MRI contrast agents, as shown in the case of Ni(II). The presence of strongly complexing and electron donating phosphonates enhances the kinetic inertness of the studied complexes and compensates the disadvantageous coordination properties of fluorine-containing ligands. Relaxation parameters of the *trans*-[Ni(te2p-tfe$_2$)]$^{2-}$ complex with fluorine atoms located about 5 Å from the Ni(II) centre are highly suitable for ^{19}F MRI hot-spot imaging employing fast pulse sequences. As the Ni(II) complexes with coordinated water molecules exhibit useful water proton T_1-relaxivity, properly designed compounds could be potentially used as dual ^{1}H/^{19}F MRI contrast agents.[29]

The work was supported by the Czech Science Foundation (P207-11-1437) and by the project of the Ministry of Health, Czech Republic, for development of research organization IN00023001 (Institutional support, Institute for Clinical and Experimental Medicine). We thank Z. Böhmová and J. Hraníček for potentiometric and AAS measurements, respectively.

Table 1 ^{19}F NMR relaxation times[a] and ^{1}H relaxivity of the studied compounds (pH 7, 25 °C)

Parameter	**1**	*cis*-[Ni(**1**)(H$_2$O)$_2$]$^{2+}$	H_4te2p-tfe$_2$	*trans*-[Ni(te2p-tfe$_2$)]$^{2-}$
B_0 = 7.05 T (300 MHz for ^{1}H, 282 MHz for ^{19}F)				
T_1(^{19}F)	0.8(3) s	1.72(1) ms	0.5(1) s	2.8(7) ms
T_2^*(^{19}F)	≈76 ms	≈0.82 ms	≈50 ms	≈0.90 ms
T_2^*/T_1(^{19}F)	0.1	0.48	0.1	0.32
r_1(^{1}H)	—	0.83(3)	—	0.18(1)
B_0 = 4.70 T (200 MHz for ^{1}H, 188 MHz for ^{19}F)				
T_1(^{19}F)	0.82(1) s	1.2(1) ms	1.1(2) s	4.2(1.1) ms
T_2^*(^{19}F)	3.1(1) ms	0.62(1) ms	3.1(2) ms	1.1(1) ms
T_2^*/T_1	0.0038	0.52	0.0028	0.26
r_1(^{1}H)	—	0.66(4) s^{-1} mM^{-1}	—	0.12(2) s^{-1} mM^{-1}

[a] T_1 was determined using inversion recovery pulse sequence; T_2^* was determined from line-width using Lorentzian-shape fitting of the signal.

References

1 *The Chemistry of Contrast Agents in Medical Magnetic Resonance Imaging*, ed. A. Merbach, L. Helm and É. Tóth, Wiley, Hoboken, 2nd edn, 2013.
2 P. Caravan, J. J. Ellison, T. J. McMurry and R. B. Lauffer, *Chem. Rev.*, 1999, **99**, 2293–2352; P. Hermann, J. Kotek, V. Kubíček and I. Lukeš, *Dalton Trans.*, 2008, 3027–3047; C. F. G. C. Geraldes and S. Laurent, *Contrast Media Mol. Imaging*, 2009, **4**, 1–23.
3 J. Ruiz-Cabello, B. P. Barnett, P. A. Bottomley and J. W. M. Bulte, *NMR Biomed.*, 2011, **24**, 114–129.
4 J. C. Knight, P. G. Edwards and S. J. Paisey, *RSC Adv.*, 2011, **1**, 1415–1425.
5 J.-X. Yu, R. R. Hallac, S. Chiguru and R. P. Mason, *Prog. Nucl. Magn. Reson. Spectrosc.*, 2013, **70**, 25–49.
6 I. Tirotta, V. Dichiarante, C. Pigliacelli, G. Cavallo, G. Terraneo and F. B. Bombelli, *Chem. Rev.*, 2015, **115**, 1106–1129.
7 S. Temme, F. Boenner, J. Schrader and U. Floegel, *Wiley Interdiscip. Rev.: Nanomed. Nanobiotechnol.*, 2012, **4**, 329–343.
8 E. T. Ahrens and J. Zhong, *NMR Biomed.*, 2013, **26**, 860–871.
9 Y. B. Yu, *Wiley Interdiscip. Rev.: Nanomed. Nanobiotechnol.*, 2013, **5**, 646–661.
10 D. Bartusik and B. Tomanek, *Adv. Drug Delivery Rev.*, 2013, **65**, 1056–1064.
11 H. Amiri, M. Srinivas, A. Veltien, M. J. van Uden, I. J. M. de Vries and A. Heerschap, *Eur. J. Radiol.*, 2015, **25**, 726–735.
12 (*a*) P. K. Senanayake, A. M. Kenwright, D. Parker and S. K. van der Hoorn, *Chem. Commun.*, 2007, 2923–2925; (*b*) A. M. Kenwright, I. Kuprov, E. De Luca, D. Parker, S. U. Pandya, P. K. Senanayake and D. G. Smith, *Chem. Commun.*, 2008, 2514–2516; (*c*) K. H. Chalmers, E. De Luca, N. H. M. Hogg, A. M. Kenwright, I. Kuprov, D. Parker, M. Botta, J. I. Wilson and A. M. Blamire, *Chem. – Eur. J.*, 2010, **16**, 134–148; (*d*) K. H. Chalmers, M. Botta and D. Parker, *Dalton Trans.*, 2011, **40**, 904–913; (*e*) P. Harvey, I. Kuprov and D. Parker, *Eur. J. Inorg. Chem.*, 2012, 2015–2022; (*f*) P. Harvey, K. H. Chalmers, E. De Luca, A. Mishra and D. Parker, *Chem. – Eur. J.*, 2012, **18**, 8748–8757; (*g*) E. De Luca, P. Harvey, K. H. Chalmers, A. Mishra, P. K. Senanayake, J. I. Wilson, M. Botta, M. Fekete, A. M. Blamire and D. Parker, *J. Biol. Inorg. Chem.*, 2014, **19**, 215–227.
13 K. H. Chalmers, A. M. Kenwright, D. Parker and A. M. Blamire, *Magn. Reson. Med.*, 2011, **66**, 931–936.
14 E. Belorizky, P. H. Fries, L. Helm, J. Kowalewski, D. Kruk, R. R. Sharp and P.-O. Westlund, *J. Chem. Phys.*, 2008, **128**, 052315.
15 A. O. Olatunde, S. J. Dorazio, J. A. Spernyak and J. R. Morrow, *J. Am. Chem. Soc.*, 2012, **134**, 18503–18505.
16 W. Curran and R. Angier, *J. Org. Chem.*, 1966, **31**, 3867–3868.
17 X. Sun, M. Wuest, Z. Kovács, A. D. Sherry, R. Motekaitis, Z. Wang, A. E. Martell, M. J. Welch and C. J. Anderson, *J. Biol. Inorg. Chem.*, 2003, **8**, 217–225.
18 C. E. McKenna, M. T. Higa, N. H. Cheung and M.-C. McKenna, *Tetrahedron Lett.*, 1977, **18**, 155–158.
19 B. Bosnich, C. K. Poon and M. Tobe, *Inorg. Chem.*, 1965, **4**, 1102–1108.
20 (*a*) K. R. Adam, I. M. Atkinson and L. F. Lindoy, *Inorg. Chem.*, 1997, **36**, 480–481; (*b*) M. Zimmer, *Coord. Chem. Rev.*, 2001, **212**, 133–163.
21 M. A. Donnelly and M. Zimmer, *Inorg. Chem.*, 1999, **38**, 1650–1658.
22 J. Kotek, P. Vojtíšek, I. Císařová, P. Hermann and I. Lukeš, *Collect. Czech. Chem. Commun.*, 2001, **66**, 363–381.
23 J. Kotek, P. Hermann, I. Císařová, J. Rohovec and I. Lukeš, *Inorg. Chim. Acta*, 2001, **317**, 324–330.
24 J. Havlíčková, H. Medová, T. Vitha, J. Kotek, I. Císařová and P. Hermann, *Dalton Trans.*, 2008, 5378–5386.
25 J. Kotek, P. Vojtíšek, I. Císařová, P. Hermann, P. Jurečka, J. Rohovec and I. Lukeš, *Collect. Czech. Chem. Commun.*, 2000, **65**, 1289–1316.
26 I. Svobodová, J. Havlíčková, J. Plutnar, P. Lubal, J. Kotek and P. Hermann, *Eur. J. Inorg. Chem.*, 2009, 3577–3592.
27 I. Svobodová, P. Lubal, J. Plutnar, J. Havlíčková, J. Kotek, P. Hermann and I. Lukeš, *Dalton Trans.*, 2006, 5184–5197.
28 J. Kotek, P. Lubal, P. Hermann, I. Císařová, I. Lukeš, T. Godula, I. Svobodová, P. Táborský and J. Havel, *Chem. – Eur. J.*, 2003, **9**, 233–248.
29 M. Wolters, S. G. Mohades, T. M. Hackeng, M. J. Post, M. E. Kooi and W. H. Backes, *Invest. Radiol.*, 2013, **48**, 341–350.

